Dynamical Analysis of the Fractional-Order Memristive Band Pass Filter Chaotic Circuit

Chenguang Ma[1,2], Xiaoqiang Yu[1,2], Feifei Yang[1,2], and Jun Mou[1,2(✉)]

[1] School of Information Science and Engineering, Dalian Polytechnic University, Dalian 116034, China
[2] School of Physics and Electronics, Central South University, Changsha 410083, China
moujun@csu.edu.cn

Abstract. In this paper, a memristive band pass filter chaotic circuit system was designed based on a band pass filter circuit. The system numerical solutions were calculated by using the Adomian decomposition (ADM) algorithm. On this basis, the dynamical characteristics of the system were analyzed by means of bifurcation diagram, Lyapunov exponent spectrum, phase diagram of chaotic attractor, Poincaré section, SE (spectral entropy) and C_0 complexity algorithm. The results of analysis show that the fractional-order memristive chaotic system has richer dynamical behaviors compared with the integer order system. This paper provides a theoretical basis for the application of fractional-order memristor chaotic circuits in the fields of secure communication and information security.

Keywords: ADM algorithm · Fractional-order system · Dynamic characteristic · Memristor chaotic circuit

1 Introduction

Memristor is the fourth basic electrical element besides resistance, capacitance and inductance. The chaotic circuit constructed by memrisor can be widely used in the fields of physics, biomedicine, secure communication and information security [1–3], so the construction of well-performing memristor chaotic circuits has attracted extensive attention of scholars [4–6]. Memristor is a device that describes the relationship between charge and magnetic flux, which is generally divided into charge-controlled memristor and magnetic-controlled memristor. The main difference is the difference in the dominant quantity, the dominant quantity of the charge-controlled memristor is the charge, and the magnetic-control memristor plays the dominant volume is the magnetic flux [7, 8]. At present, although commercial memristor has not yet begun to be applied, the study of equivalent circuit to achieve the function of memristor has been vigorously carried out. So far, many chaotic circuits based on memristor have been proposed. Among them, Ye et al. designed a hyperchaotic system based on the Venn-bridge self-oscillating circuit, and analyzed the dynamic characteristics of the system by using SE and C_0 complexity algorithms [9]. A hyperchaotic memristor circuit based on Lorentz

© ICST Institute for Computer Sciences, Social Informatics and Telecommunications Engineering 2019
Published by Springer Nature Switzerland AG 2019. All Rights Reserved
J. Jin et al. (Eds.): GreeNets 2019, LNICST 282, pp. 181–192, 2019.
https://doi.org/10.1007/978-3-030-21730-3_20

system was constructed by Ruan et al. and its dynamical characteristics was analyzed [10]. Compared with integer order memristor chaotic system, fractional-order memristor chaotic system often has more complex dynamic characteristics. In recent years, the research on fractional-order memristor chaotic systems has become a hot topic. The definition of fractional calculus mainly includes Riemann-Liouville and Caputo. Up to now, there are three main methods to solve fractional-order chaotic systems, namely frequency-domain analysis [11], predictive correction [12] (ABM) and Adomian [13] algorithm (ADM). Among them, ADM algorithm has the superiority like high accuracy, fast convergence, does not need discrete processing, and occupies less computer memory. So ADM algorithm is widely used in the analysis of fractional-order chaotic systems. Sun et al. made a detailed analysis of the dynamic characteristics of fractional-order simplified unified chaotic system by means of direct observation of phase diagram, calculation of power spectrum and other methods [14]. Numerical solution of the fractional-order diffusionless Lorentz system was analyzed by He and others using ADM algorithm. [15]. Xu et al. used ADM algorithm to analyze the dynamic characteristics of simplified unified fractional-order chaotic system [14]. These studies show that fractional-order chaotic systems usually have more complex dynamic characteristic than integer-order chaotic systems. And the SE and C_0 complexity algorithms can be used to evaluate the randomness of the system [15, 16]. Bao et al. designed a simple third-order memristor chaotic circuit and analyzed its chaotic characteristics in detail [17], but the fractional-order system is not analyzed. Therefore, based on this circuit, a new fractional-order memristor band-pass filter chaotic circuit system is designed and its dynamic characteristics are analyzed in detail in this paper.

In this paper, the dynamic characteristics of fractional-order memristor band pass filter chaotic circuits are analyzed. In the first part, a fractional-order memristor chaotic circuit is defined based on the third-order memristor band pass filter chaotic circuit. The second part describes the ADM algorithm in detail, and analyzes the parameter iterative relation of fractional-order memristor chaotic circuit, as well as the numerical accurate solution of the system. In the third part, the dynamic characteristics of the fractional-order system are analyzed. The fourth part is the conclusion.

2 Memristive BPF Chaotic Circuit System

An improved charge-controlled memristor equivalent circuit is shown in Fig. 1, which is composed of a capacitor, two multipliers, three resistors and two op-amplifiers. V and I represent the voltage and current at the input port, respectively. V_0 represents the voltage across the integral capacitor C_0, and g is the proportional coefficient between the multipliers. The memristor can be expressed as:

$$\begin{cases} i = W(V_0)v = \frac{1}{R_c}(1 - gV_0^2)v \\ \frac{dV_0}{dt} = f(V_0, v) = -\frac{1}{R_b C_0}V_0 - \frac{1}{R_a C_0}v \end{cases} \tag{1}$$

Figure 2(a) shows a band-pass filter circuit consisting of 4 resistors, 2 capacitors and an op-amplifier. The filter circuit is similar to a typical Venn oscillating circuit, but

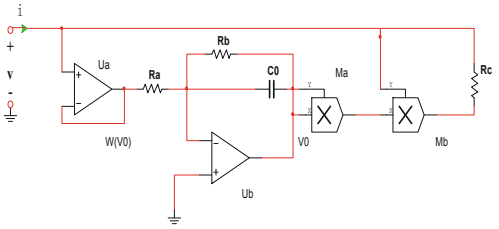

Fig. 1. Improved charge-controlled memristor

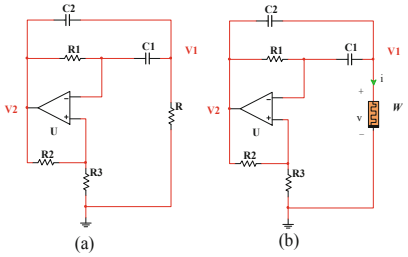

Fig. 2. BPF chaotic circuit and memristive BPF chaotic circuit

the topological structure is different. Replace the resistor R in Fig. 2(a) with the improved charge-controlled memristor W shown in Fig. 1, the chaotic circuit of memristive band-pass filter as shown in Fig. 2(b) will obtained. The third-order memristor chaotic circuit consists of 6 resistors, 3 op-amplifiers, 3 capacitors and 2 multipliers.

According to the model of memristor and the memristor circuit, based on Kirchhoff's law and ohm's law, the circuit equation of the system can be obtained as:

$$\begin{cases} \frac{dV_0}{dt} = -\frac{1}{R_b C_0} V_0 - \frac{1}{R_a C_0} V_1 \\ \frac{dV_1}{dt} = \frac{1-gV_0^2}{(k-1)R_c C_2} V_1 - \frac{1}{R_1}\left(\frac{1}{C_1} + \frac{1}{kC_2}\right) V_2 \\ \frac{dV_2}{dt} = \frac{k(1-gV_0^2)}{(k-1)R_c C_2} V_1 - \frac{1}{R_1}\left(\frac{1}{C_1} + \frac{1}{C_2}\right) V_2 \end{cases}, \tag{2}$$

Where, $k = 1 + R_2/R_3$, V_0, V_1, V_2 are the potentials of the three nodes in the circuit, let $x = V_0$, $y = V_1$, $z = V_2$, $u = du/d\tau$ ($u \equiv x, y, z$), $C_1 = C_2 = C$, $\tau = t/R_1C$, $a = R_1C/R_bC_0$, $b = R_1C/R_aC_0$, $c = R_1/R_c$. By substituting them into Eq. (2) and doing dimensionless processing of the circuit parameters, the dimensionless system equation can be obtained as:

$$\begin{cases} \dot{x} = -ax - by \\ \dot{y} = c(1 - gx^2)y/(k-1) - (k+1)z/k \\ \dot{z} = kc(1 - gx^2)y/(k-1) - 2z \end{cases}. \tag{3}$$

Let $a = 8$, $b = 80$, $c = 500/3$, $g = 0.1$, $k = 21$. The attractor phase diagram is shown in Fig. 3. The Lyapunov exponents of the system is (1.0893, 0, −6.2240), while the Lyapunov dimension $D_L = 2.175$, which indicates that the system is in chaotic state.

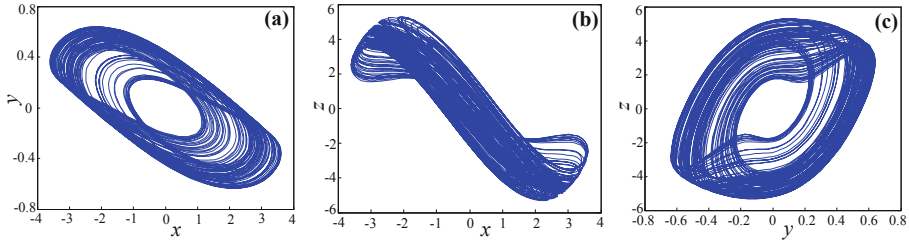

Fig. 3. Attractor phase diagram (a) x-y plane, (b) x-z plane, (c) y-z plane

3 Numerical Analysis of Fractional-Order Memristor Chaotic Circuit

3.1 Adomian Decomposition Algorithm

For a certain fractional-order chaotic system ${}_*D_{to}^q x(t) = f(x(t)) + g(t)$. where, $x(t) = [x_1(t), x_2(t), \ldots, x_n(t)]^{\mathrm{T}}$ is the system state variable. For a autonomous systems, $g(t) = [g_1(t), g_2(t), \ldots, g_n(t)]^{\mathrm{T}}$ is a constant. $f(x(t))$ contains linear part and nonlinear part. Then, the system equation can be decomposed into:

$$\begin{cases} {}^*D_{t_0}^q x(t) = Lx(t) + Nx(t) + g(x(t)) \\ x^{(k)}(t_0^+) = b_k, k = 0, 1, 2 \cdots m-1, \\ m \in N, m-1 < q \le m \end{cases} \tag{4}$$

Where, ${}^*D_{to}^q$ is a q-order Caputo differential operator, and L and N are the linear and nonlinear parts of the system respectively. The b_k is the initial value. The solutions of equations as follows can be obtained after applying Riemann-Liouville fractional integral operator J_{to}^q on both sides of the equations.

$$x = J_{t_0}^q Lx + J_{t_0}^q Nx + J_{t_0}^q g + \sum_{k=0}^{m-1} \frac{(t-t_0)^k}{k!}. \tag{5}$$

According to the principle of Adomian decomposition method, the nonlinear part can be decomposed into:

$$A_{\mathrm{j}}^{\mathrm{i}} = \frac{1}{i!}\left[\frac{d^i}{d\lambda^i} N\left(\sum\nolimits_{k=0}^{i} (\lambda)^k x_j^k\right)\right]_{\lambda=0}, \tag{6}$$

Where, $i = 0, 1, \ldots, j = 0, 1, \ldots n$. Thus, the nonlinear term can be expressed as:

$$Nx = \sum_{i=0}^{\infty} A^i(x^0, x^1, x^2, \ldots, x^i), \tag{7}$$

Therefore, the solution of Eq. (4) is:

$$x = \sum_{i=0}^{\infty} x^i = J_{t_0}^q L \sum_{i=0}^{\infty} x^i + J_{t_0}^q \sum_{i=0}^{\infty} A^i + J_{t_0}^q g + \sum_{k=0}^{m-1} \frac{(t-t_0)^k}{k!}. \tag{8}$$

And its operation relation is:

$$\begin{cases} x^0 = J_{t_0}^q g + \sum\limits_{k=0}^{m-1} \frac{(t-t_0)^k}{k!} \\ x^1 = J_{t_0}^q L x^0 + J_{t_0}^q A^0(x^0) \\ x^2 = J_{t_0}^q L x^1 + J_{t_0}^q A^1(x^0, x^1) \\ \ldots \\ x^i = J_{t_0}^q L x^{i-1} + J_{t_0}^q A^{i-1}(x^0, x^1, \ldots, x^{i-1}) \end{cases}. \tag{9}$$

3.2 Numerical Solutions to the System Equations

From the system (3), the system equation of the fractional-order memristor chaotic circuit can be obtained by

$$\begin{cases} {}^*D_{t_0}^q x_1 = -a x_1 - b x_2 \\ {}^*D_{t_0}^q x_2 = c(1 - g x_1^2) x_2/(k-1) - (k+1) x_3/k, \\ {}^*D_{t_0}^q x_3 = kc(1 - g x_1^2) x_2/(k-1) - 2 x_3 \end{cases} \tag{10}$$

Where, q is the order of the system, x, y and z represent the state variable of the system. Based on the Adomian algorithm, the linear and nonlinear parts of the system can be decomposed as:

$$\begin{bmatrix} Lx_1 \\ Lx_2 \\ Lx_3 \end{bmatrix} = \begin{bmatrix} -a x_1 - b x_2 \\ c x_2/(k-1) - (k+1) x_3/k \\ kc x_2/(k-1) - 2 x_3 \end{bmatrix}, \quad \begin{bmatrix} Nx_1 \\ Nx_2 \\ Nx_3 \end{bmatrix} = \begin{bmatrix} 0 \\ -d x_1^2 x_2 \\ -kd x_1^2 x_2 \end{bmatrix}, \quad \begin{bmatrix} g_1 \\ g_2 \\ g_3 \end{bmatrix} = \begin{bmatrix} 0 \\ 0 \\ 0 \end{bmatrix} \tag{11}$$

Where, $d = cg/(k-1)$. Therefore:

$$A_2 = -dx_1^2 x_2, A_3 = -kdx_1^2 x_2 \tag{12}$$

The nonlinear term $x_1^2 x_2$ is decomposed according to the Eq. (6), and the first 5 items are intercepted on the premise of ensuring the calculation accuracy, which can be expressed as:

$$\begin{cases} A_2^0 = -x_2^0 (x_1^0)^2, \\ A_2^1 = -x_2^1 (x_1^0)^2 - 2x_2^0 x_1^1 x_1^0, \\ A_2^2 = -x_2^2 (x_1^0)^2 - 2x_2^1 x_1^1 x_1^0 - 2x_2^0 x_1^2 x_1^0 - x_2^0 (x_1^1)^2, \\ A_2^3 = -x_2^3 (x_1^0)^2 - 2x_2^2 x_1^1 x_1^0 - x_2^1 (x_1^1)^2 - 2x_2^1 x_1^2 x_1^0 - 2x_2^0 x_1^3 x_1^0 - 2x_2^0 x_1^1 x_1^2, \\ A_2^4 = -x_2^4 (x_1^0)^2 - 2x_2^3 x_1^1 x_1^0 - x_2^2 (x_1^1)^2 - 2x_2^2 x_1^2 x_1^0 - 2x_2^1 x_1^2 x_1^1 - 2x_2^1 x_1^3 x_1^0 - 2x_2^0 x_1^4 x_1^0 - 2x_2^0 x_1^3 x_1^1 - x_2^0 (x_1^2)^2 \end{cases} \tag{13}$$

$$\begin{cases} A_3^0 = -x_2^0 (x_1^0)^2, \\ A_3^1 = -x_2^1 (x_1^0)^2 - 2x_2^0 x_1^1 x_1^0, \\ A_3^2 = -x_2^2 (x_1^0)^2 - 2x_2^1 x_1^1 x_1^0 - 2x_2^0 x_1^2 x_1^0 - x_2^0 (x_1^1)^2, \\ A_3^3 = -x_2^3 (x_1^0)^2 - 2x_2^2 x_1^1 x_1^0 - x_2^1 (x_1^1)^2 - 2x_2^1 x_1^2 x_1^0 - 2x_2^0 x_1^3 x_1^0 - 2x_2^0 x_1^1 x_3^2, \\ A_3^4 = -x_2^4 (x_1^0)^2 - 2x_2^3 x_1^1 x_1^0 - x_2^2 (x_1^1)^2 - 2x_2^2 x_1^2 x_1^0 - 2x_2^1 x_1^2 x_1^1 - 2x_2^1 x_1^3 x_1^0 - 2x_2^0 x_1^4 x_1^0 - 2x_2^0 x_1^3 x_1^1 - x_2^0 (x_1^2)^2. \end{cases} \tag{14}$$

$$\begin{cases} x_1^1 = (-ax_1^0 - bx_2^0) \frac{(t-t_0)^q}{\Gamma(q+1)} \\ x_2^1 = [c(1 - g(x_1^0)^2) x_2^0/(k-1) - (k+1)x_3^0/k] \frac{(t-t_0)^q}{\Gamma(q+1)} \\ x_3^1 = [kc(1 - g(x_1^0)^2) x_2^0/(k-1) - 2x_3^0] \frac{(t-t_0)^q}{\Gamma(q+1)} \end{cases} \tag{15}$$

Equation (17) is obtained from the initial conditions, where $x_j^0 (j = 1, 2, 3)$ is the initial value of the system (4) and $h = t - t_0$. Similarly, the remaining three terms can be obtained, so the numerical solution of the system is

$$\tilde{x}_j(t) = x_j^0 + x_j^1 + x_j^2 + x_j^3 + x_j^4 \tag{16}$$

Let

$$\begin{cases} c_1^0 = x_1^0 \\ c_2^0 = x_2^0 \\ c_3^0 = x_3^0 \end{cases} \tag{17}$$

$$\begin{cases} c_1^1 = -ac_1^0 - bc_2^0, \\ c_2^1 = cc_2^0/(k-1) - (k+1)c_3^0/k - dc_2^0 (c_1^0)^2 \\ c_3^1 = kcc_2^0/(k-1) - 2c_3^0 - kdc_2^0 (c_1^0)^2 \end{cases} \tag{18}$$

$$\begin{cases} c_1^2 = -ac_1^1 - bc_2^1 \\ c_2^2 = cc_2^1/(k-1) - (k+1)c_3^1/k - d[c_2^1(c_1^0)^2 - 2c_2^0c_1^1c_1^0] \\ c_3^2 = kcc_2^1/(k-1) - 2c_3^1 - kd[c_2^1(c_1^0)^2 - 2c_2^0c_1^1c_1^0] \end{cases} \tag{19}$$

$$\begin{cases} c_1^3 = -ac_1^2 - bc_2^2, \\ c_2^3 = cc_2^2/(k-1) - (k+1)c_3^2/k - dc_2^2(c_1^0)^2 - d[(2c_2^1c_1^1c_1^0 + c_2^0(c_1^1)^2)\frac{\Gamma(2q+1)}{\Gamma^2(q+1)} + 2c_2^0c_1^2c_1^0] \\ c_3^3 = kcc_2^2/(k-1) - 2c_3^2 - kdc_2^2(c_1^0)^2 - kd[(2c_2^1c_1^1c_1^0 + c_2^0(c_1^1)^2)\frac{\Gamma(2q+1)}{\Gamma^2(q+1)} + 2c_2^0c_1^2c_1^0] \end{cases} \tag{20}$$

$$\begin{cases} c_1^4 = -ac_1^3 - bc_2^3 \\ c_2^4 = cc_2^3/(k-1) - (k+1)c_3^3/k - d[c_2^3(c_1^0)^2 + 2c_2^0c_1^3c_1^0 + c_2^1(c_1^1)^2\frac{\Gamma(3q+1)}{\Gamma^3(q+1)}] \\ \qquad + (2c_2^2c_1^1c_1^0 + 2c_2^1c_1^2c_1^0 + 2c_2^0c_1^1c_1^2)\frac{\Gamma(3q+1)}{\Gamma(2q+1)\Gamma(q+1)} \\ c_3^4 = kcc_2^3/(k-1) - 2c_3^3 - kd[c_2^3(c_1^0)^2 + 2c_2^0c_1^3c_1^0 + c_2^1(c_1^1)^2\frac{\Gamma(3q+1)}{\Gamma^3(q+1)}] \\ \qquad + (2c_2^2c_1^1c_1^0 + 2c_2^1c_1^2c_1^0 + 2c_2^0c_1^1c_1^2)\frac{\Gamma(3q+1)}{\Gamma(2q+1)\Gamma(q+1)} \end{cases} \tag{21}$$

Therefore, the Eq. (16) is same as Eq. (22) as follow:

$$\tilde{x}_j(t) = c_j^0 + c_j^1\frac{(t-t_0)^q}{\Gamma(q+1)} + c_j^2\frac{(t-t_0)^{2q}}{\Gamma(2q+1)} + c_j^3\frac{(t-t_0)^{3q}}{\Gamma(3q+1)} + c_j^4\frac{(t-t_0)^{4q}}{\Gamma(4q+1)} \tag{22}$$

In the process of solving, the integral interval needs to be divided into small sections (t_k, t_{k+1}), and the result obtained will be the initial value of the next section (t_{k+1}, t_{k+2}). Let $h = (t_k - t_{k-1})$, a total of $(t_{k+1} - t_k)/(h-1)$ iterations is required.

4 Dynamic Analysis of Fractional-Order Memristor Chaotic Circuits

4.1 The Influence of Parameter *a* on the Dynamic Characteristics of the System

Let $q = 0.9$, and initial value $x_0 = [0, 0.000006, 0]$, $h = 0.001$, the phase diagram of the system is shown in Fig. 4. In this point the Lyapunov exponent is (1.8255, 0, −12.9251), with the Lyapunov dimension $D_L = 2.14$. The system is in a chaotic state at this time, due to a positive Lyapunov exponent. And the maximum Lyapunov exponent is larger than the maximum Lyapunov exponent of integer order. So the system has more complex chaotic characteristics.

If $q = 0.9$, the bifurcation diagram of the system when a changes from 7 to 11 is shown in Fig. 5(a). It can be seen from the bifurcation diagram that, when the parameters $a \in (7, 7.172)$ and $a \in (8.925, 11)$, the system is in a periodic state. However, when $a \in (7.172, 8.925)$, the system is in a chaotic state.

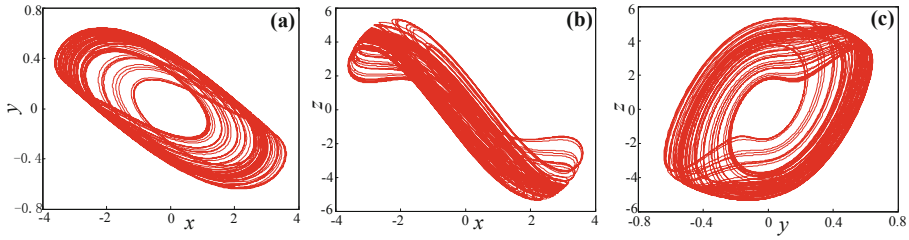

Fig. 4. Attractor phase diagram of system with $a = 8$ and $q = 0.9$ (a) x-y plane, (b) x-z plane, (c) y-z plane

Based on the ADM algorithm, QR decomposition method is used to calculate the Lyapunov exponent spectrum of the system varying with parameter a, as shown in Fig. 5(b). It can be seen from the figure that when $a \in (7.172, 8.925)$, the Lyapunov exponent of the system is positive and the system is in a chaotic state, which is corresponding to the bifurcation diagram. In particular, when $7.809 < a < 7.875$, the Lyapunov exponent of the system is small and the randomness of chaotic sequence is weak. The maximum Lyapunov exponent of the fractional order is greater than 2, while the maximum Lyapunov exponent of the integer order is less than 2. Therefore, the dynamic characteristics of the fractional order chaotic system are better than that of the corresponding integer order chaotic system.

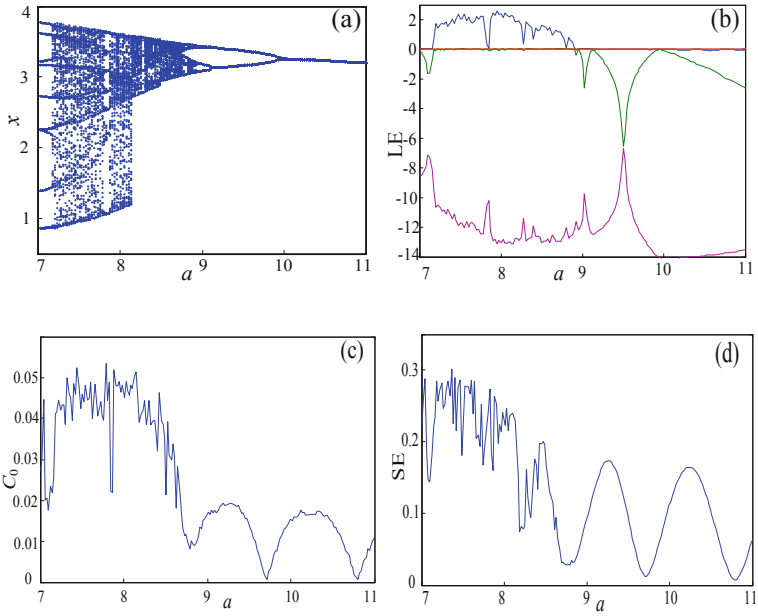

Fig. 5. The system varies with parameter a (a) Bifurcation diagram, (b) Lyapunov exponent spectrum, (c) C_0 complexity, (d) SE complexity

In order to further characterize the dynamic characteristics of the chaotic system, SE and C_0 complexity algorithms were used to obtain the complexity of the system varying with parameter a, as shown in Fig. 5(c) and (d). When $a \in (7.172, 8.9)$, system is periodic state, both SE and C_0 values are small. And when the system enters chaotic state, the complexity of the system increases and the fluctuation amplitude is large. The system enters the periodic state again when a in the (8.9, 11). In this time SE and C_0 both change gently and gradually approach 0, which indicate the complexity of system' sequence decreases, that is, the randomness of chaotic sequence decreases.

4.2 Dynamic Characteristics of the System Varying with Order q

Set $a = 8$, q varying from 0.5 to 1, and keep other parameter values unchanged, the bifurcation diagram of the system is shown in Fig. 6(a). As can be seen from Fig. 6(a), when $q > 0.709$, the system enters a chaotic state through period-doubling bifurcation. Figure 6(b) shows the Lyapunov exponent spectrum of the system changing with the order q. Chaos characteristics of the system are mainly affected by the maximum Lyapunov exponent, so in order to show clarity, the minimum Lyapunov exponent curve is omitted from Fig. 6(b). It can also be seen from the Fig. 6(b) that the Lyapunov exponent increases with the increase of order q, and the minimum order of chaos generation is 0.709, which is completely corresponding to the bifurcation diagram.

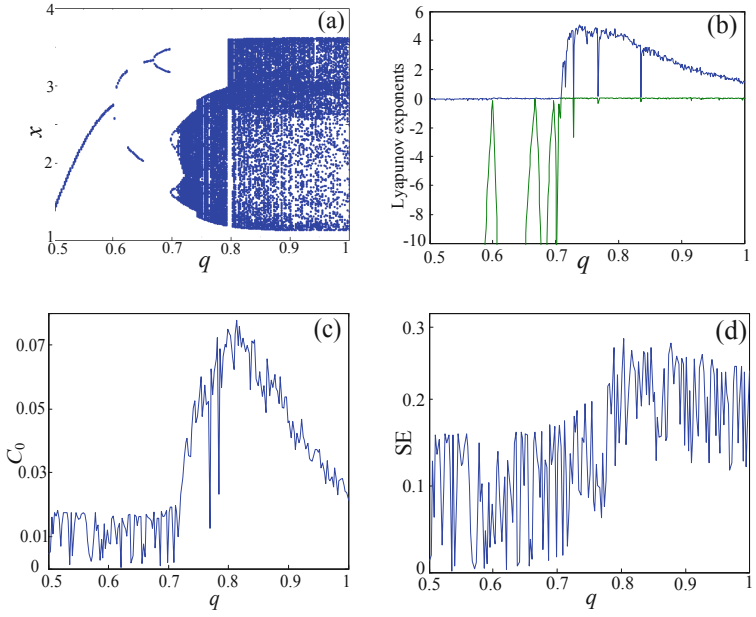

Fig. 6. The system varies with parameter q (a) Bifurcation diagram, (b) Lyapunov exponent spectra (c) C_0 complexity, (d) SE complexity

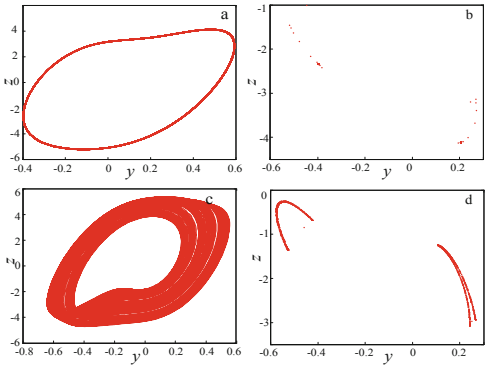

Fig. 7. Phase diagram and Poincaré section of the system in the y-z plane (a) Phase diagram of system on the y-z plane when $a = 8$, $q = 0.65$; (b) Poincaré section on the y-z plane when $a = 8$, $q = 0.65$; (c) Phase diagram of system on the y-z plane when $a = 8$, $q = 0.8$; (d) Poincaré section on the y-z plane when $a = 8$, $q = 0.65$

To further analyze the dynamic characteristics of the system, the C_0 and SE complexity of the system when the order q changes is analyzed, as shown in Fig. 6(c) and (d). It can be seen from the figure that when $0.5 < q < 0.709$, the system complexity is low, and when $q > 0.709$, the system enters the chaotic state system and the complexity increases, and the dynamic characteristics of the system are more complex.

The Fig. 7 shows the phase diagram of the system in the y-z plane and the Poincaré section of the y-z in the plane $x = 1$ when $a = 8$, $q = 0.65$ and $a = 8$, $q = 0.8$. When $a = 8$ and $q = 0.65$, the phase diagram of the system shows a limit cycle and the Poincaré section shows limit discrete point. When $a = 8$ and $q = 0.8$, chaotic attractors appear in the system. Poincaré section is the dense point of fractal structure, which corresponds to the bifurcation graph and Lyapunov exponent spectrum.

4.3 Dynamic Characteristics of the System When Parameters *a* and Order *q* Change Simultaneously

Let the initial value be $x_0 = [0, 0.000006, 0]$, $h = 0.001$, and keep other parameter values unchanged. Based on SE and C_0 algorithms, 2D SE and C_0 complexity contour lines can be obtained, as shown in Fig. 8(a) and (b). This figure represents the complexity of the system with different parameter a and q, and provides a reference for selecting appropriate system parameters and order numbers for better application. In Fig. 8, different colors indicate different complexity. The darker the color represents the higher the complexity and the higher the randomness of chaotic sequences. The maximum complexity of SE is 0.3712, corresponding $a = 7$, $q = 0.8243$, and the maximum Lyapunov exponent is 3.419. The maximum complexity of C_0 is 0.1113, $a = 7$, $q = 0.7207$, and the maximum Lyapunov exponent is 6.3243. It should be pointed out that when $a = 7$, $0.7207 < q < 0.8$, C_0 complexity is small, and in practical

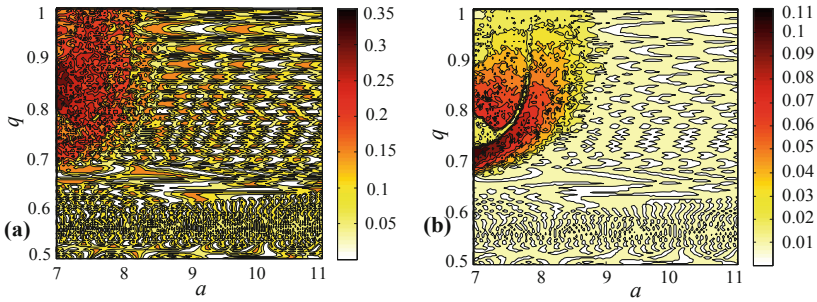

Fig. 8. Complexity of the system varying with parameters a and order q (a) 2D SE complexity, (b) 2D C_0 complexity

applications should avoid taking values in this range. In general, when $a = 7$, $0.8 < q < 0.9$, chaos sequences within the range of this region should be selected as far as possible because the system has a good stochastic performance.

5 Conclusion

In this paper, a novel memristor band pass chaotic filter circuit is constructed and the numerical solution of fractional-order memristor chaotic circuit is calculated based on Adomian algorithm. The dynamic characteristics of the system are analyzed by means of phase diagram, Poincaré section, bifurcation diagram, Lyapunov exponent spectrum, SE and C_0 complexity algorithms. The results show that the dynamical characteristics of fractional-order memristor band pass chaotic circuit system are more complex than its corresponding integer order system and more suitable for the application of secure communication and other fields. When $a = 7$, $0.8 < q < 0.9$, the system chaotic sequence has the best randomness and the highest security. The research results of this paper provide a theoretical basis for the application of memristor band pass filter chaotic circuit in secure communication and other fields and have high theoretical and application value.

References

1. Joglekar, Y.N., Wolf, S.J.: The elusive memristor: signatures in basic electrical circuits (2008)
2. Mou, J., Li, P., Wang, J., et al.: Synchronization study of chaotic system and study in the security communication. ICIC Express Lett. **6**(9), 2325–2330 (2012)
3. Yang, S., Li, C., Huang, T.: Impulsive control and synchronization of memristor-based chaotic circuits. Int. J. Bifurc. Chaos **24**(12), 1450162 (2014)
4. Bao, B., Ma, Z., Jianping, X., et al.: A simple memristor chaotic circuit with complex dynamics. Int. J. Bifurc. Chaos **21**(09), 1102999 (2011)
5. Wang, W., Wang, G., Tan, D.: A new memristor based chaotic circuit. In: International Workshop on Chaos-Fractals Theories and Applications (2011)

6. Saini, S., Saini, J.S.: Secure communication using memristor based chaotic circuit. In: International Conference on Parallel (2015)
7. Buscarino, A., Fortuna, L., Frasca, M., et al.: A chaotic circuit based on Hewlett-Packard memristor. Chaos Interdiscip. J. Nonlinear Sci. **22**(2), 80–83 (2012)
8. Chandia, K.J., Bologna, M., Tellini, B.: Multiple scale approach to dynamics of an LC circuit with a charge-controlled memristor. IEEE Trans. Circ. Syst. II Express Briefs **65**(1), 120–124 (2017)
9. Ye, X., Mou, J., Luo, C., et al.: Dynamics analysis of Wien-bridge hyperchaotic memristive circuit system. Nonlinear Dyn. **92**, 923–933 (2018)
10. Jing-Ya, R., Ke-Hui, S., Jun, M.: Memristor-based Lorenz hyper-chaotic system and its circuit implementation. Acta Phys. Sin. **65**, 190502 (2016)
11. Charef, A., Sun, H.H., Tsao, Y.Y., et al.: Fractal system as represented by singularity function. IEEE Trans. Autom. Control **37**(9), 1465–1470 (2002)
12. Sun, H., Abdelwahab, A., Onaral, B.: Linear approximation of transfer function with a pole of fractional power. IEEE Trans. Autom. Control **29**(5), 441–444 (1984)
13. He, S., Sun, K., Wang, H.: Dynamics of the fractional-order Lorenz system based on Adomian decomposition method and its DSP implementation. IEEE/CAA J. Autom. Sin. 1–6 (2017)
14. Xu, Y., Sun, K., He, S., et al.: Dynamics of a fractional-order simplified unified system based on the Adomian decomposition method. Eur. Phys. J. Plus **131**(6), 1–12 (2016)
15. He, S., Sun, K., Banerjee, S.: Dynamical properties and complexity in fractional-order diffusionless Lorenz system. Eur. Phys. J. Plus **131**(8), 254 (2016)
16. He, S., Sun, K., Wang, H.: Complexity analysis and DSP implementation of the fractional-order Lorenz hyperchaotic system. Entropy **17**(12), 8299–8311 (2015)
17. Bao, B., Wang, N., Xu, Q., et al.: A simple third-order memristive band pass filter chaotic circuit. IEEE Trans. Circuits Syst. II Express Briefs **64**(8), 977–979 (2017)